Synthesis, X-ray Structure, Spectroscopic Characterization, and Theoretical Prediction of the Structure and Electronic Spectrum of Eu(btfa)$_3$·bipy and an Assessment of the Effect of Fluorine as a β-Diketone Substituent on the Ligand−Metal Energy Transfer Process

Hélcio J. Batista,[†] Antônio V. M. de Andrade,[‡] Ricardo L. Longo,[†] Alfredo M. Simas,[†] Gilberto F. de Sá,*[,†] Nao K. Ito,[§] and Larry C. Thompson[§]

Departamento de Química Fundamental and Departamento de Engenharia Química, Universidade Federal de Pernambuco, CEP 50740-540, Recife, PE, Brazil, and Department of Chemistry, University of Minnesota−Duluth, Duluth, Minnesota

Received December 26, 1997

The 2,2′-dipyridyl adducts of two europium β-diketonate complexes, Eu(btfa)$_3$·bipy [btfa = 4,4,4-trifluoro-1-phenyl-2,4-butanedione, bipy = 2,2′-dipyridyl] and Eu(bzac)$_3$·bipy [bzac = 1-phenyl-2,4-butanedione], have been prepared. The crystal structure of the former with chemical formula $EuC_{40}H_{26}O_6N_2F_9$ has been solved by single-crystal X-ray diffraction methods. The complex crystallizes in the monoclinic space group $P2_1/n$ with $a = 11.122(5)$ Å, $b = 22.860(8)$ Å, $c = 15.870(6)$ Å, $\beta = 102.62(3)^o$, $V = 3937(5)$ Å^3, and $Z = 4$. A single, eight-coordinate environment, which approximates a square antiprism, is found for the europium(III). The UV absorption spectra of both complexes were obtained from ethanol solutions and, in the case of Eu(btfa)$_3$·bipy, from a thin film. In both cases the absorption spectra are reasonably well predicted by the INDO/S-CI method using, for Eu(btfa)$_3$·bipy, both the X-ray data and that obtained through the SMLC/AM1 method as input geometry and, for Eu(bzac)$_3$·bipy, that obtained through the SMLC/AM1 method. There is a blue shift of the calculated spectra relative to the solution spectra and a slightly larger blue shift compared to the spectrum of the thin film. Both complexes are luminescent under near-UV excitation, and the spectra are in accord with the existence of a single emitting site in each. The increased quantum yield in the fluorinated complex is correlated with a decrease in the bipy−europium(III) distance, a closer match of the lowest ligand-centered triplet state (that level which is primarily responsible for the energy transfer from the ligands to the europium(III)), and the lower vibrational energy of the C−F bonds relative to the C−H bonds. In the fluorinated complex the calculations show that the lowest triplet level is primarily localized on the 2,2′-dipyridyl whereas in the nonfluorinated complex this is the second lowest triplet level.

Introduction

The rare earth β-diketone complexes have had a long and useful history.[1] The first serious, intensive study of these complexes was primarily involved in considering their use as complexing agents for separations although their interesting luminescence properties had been reported previously. For several years beginning about 1960 there was an intense effort directed toward finding suitable complexes that could be utilized in lasers. Although much of this work involved the study of materials of dubious purity and formulation, the period culminated in two definitive publications that demonstrated the types of complexes that could be formed.[2,3] The most useful of these are the tris complexes, the tetrakis complexes, and, perhaps the most useful of all, the adducts of the tris complexes. In solution these latter are most commonly manifested in the so-called "shift reagents", and during the 1970s a number of solid adducts were studied by X-ray methods in order to obtain structural information in support of various ideas relative to the mechanism of this effect.[4]

Since 1985 there has been renewed interest in these tris adducts because of a number of characteristics that make them quite useful and the fact that they can be used as precursors to other materials.[5] The number of types of molecules that can form adducts with the tris-β-diketonates is quite large and includes heterocyclic nitrogen donors such as pyridine, 2,2′-dipyridyl, 1,10-phenanthroline, and 2,2′:6′,2″-terpyridine as well as oxygen donors such as water, dimethyl sulfoxide, dimethyl formamide, and triphenylphosphine oxide, among others. In general the complexes with europium(III) and terbium(III) are strongly luminescent when excited with near-UV radiation, and the energy transfer process is highly efficient. Moreover, these adducts can generally be prepared in good purity, and it is often possible to isolate X-ray quality crystals for structure determinations. Although the luminescence spectra are definitive for the identification of a particular compound, the low symmetry does

[†] Departamento de Química Fundamental, Universidade Federal de Pernambuco.

[‡] Departamento de Engenharia Química, Universidade Federal de Pernambuco.

[§] Department of Chemistry, University of Minnesota−Duluth.

(1) Thompson, L. C. In *Handbook on the Physics and Chemistry of Rare Earths*; Gschneider, K. A., Eyring, L., Eds.; North-Holland: Amsterdam, 1979; Chapter 25.

(2) Melby, L. R.; Rose, N. J.; Abramson, E.; Caris, J. C. *J. Am. Chem. Soc.* **1964**, *86*, 5117.

(3) Bauer, H.; Blanc, J.; Ross, D. L. *J. Am. Chem. Soc.* **1964**, *86*, 5125.

(4) Sievers, R. E., Ed. *Nuclear Magnetic Shift Reagents*; Academic Press: New York 1973.

(5) Baxter, I.; Draker, S. R.; Hursthouse, M. B.; Abdyl Malik, K. M.; McAleese, J.; Otway, D. J.; Plakatouras, J. C. *Inorg. Chem.* **1995**, *34*, 1384.

S0020-1669(97)01602-9 CCC: $15.00
Published on Web 06/10/1998

not permit conclusions to be drawn about the geometry of the complex.

The variety of β-diketones and adducting molecules that are available permits the study of varying steric and electronic effects on the structure, luminescence, and efficiency of luminescence, which are of particular importance in the context of connecting modern theoretical ideas to discrete complexes. For example, the availability of complexes of known structure has enabled the theories related to band intensities and crystal field parameters to be tested and extended.[6]

Given the importance of lanthanide complexes as shift reagents and their subsequent development as contrast agents for use in magnetic resonance imaging, several molecular mechanics methods have been developed[7−10] to predict the molecular structure of such compounds. Despite the fact that these methods are computationally efficient, allowing them to be applied in molecular dynamics simulations,[10] their parametrization is very demanding and specific, limiting their application to selected groups of ligands. In addition, these methods cannot provide reliable results for bond formation/breaking in the ligand part of the complex nor of their electron density. In order to solve some of these drawbacks a molecular orbital model (sparkle model for lanthanide complexes based on Austin model 1:SMLC/AM1)[11,12] has been developed to determine the molecular and electronic structure of lanthanide compounds. This SMLC/AM1 method has proven to yield excellent geometry for large europium compounds,[11−14] including cryptate and cagelike ligands.[15] This approach has been extended and generalized for other lanthanide ions[16] as well as for the prediction of properties other than geometry, such as vibrational frequencies and intensities, enthalpy, entropy, heat capacity, etc.[17,18] In this semiempirical method the lanthanide(III) ion is replaced by a sparkle[19] with charge +3, and thus the method considers the ligand−lanthanide interaction as essentially electrostatic, keeping, however, the excellent performance of the AM1 method for the ligands and their interactions.

The molecular structure determination is the first step in the rationalization and prediction of the luminescent properties of these lanthanide compounds. The combination of the SMLC/AM1 method for obtaining molecular structure with semiempirical methods for electronic spectra calculations, such as the INDO/S-CI (intermediate neglect of differential overlap/spectroscopic−configuration interaction) method,[20,21] has provided a valuable theoretical tool to study the effects of the ligands on the luminescent properties. The energy levels and transition moments, as well as other electronic properties determined by these combined methodologies, have been used to estimate the rate of energy transfer between the ligands and the Ln(III) ion, allowing the calculation of the quantum yield for the luminescence processes.[22]

The ultimate aim of our work is to use these powerful predictive tools to design ligands which will form stable complexes that will function as efficient light conversion molecular devices (LCMD). Such complexes should have strong ligand-centered absorption in the UV region, efficient ligand to metal energy transfer rates, and intense metal-centered emission in the visible range, red for Eu(III) or green for Tb(III). Toward this end it is important to test further the utility of the predictive theoretical methods on a series of compounds in which it is possible to vary both steric and electronic effects. As pointed out above, the adducts of the tris-β-diketone complexes are an excellent choice for these tests and, consequently, in this communication the synthesis, structure, and absorption and luminescence spectra of Eu(btfa)$_3$·bipy are reported together with the results of both types of calculations. Similar calculations are made for the corresponding benzoylacetone complex in order to compare the efficiency of emission between the fluorinated and nonfluorinated compounds. This fluorinated complex was chosen for these studies, in part, because it is sufficiently volatile that it can be deposited as thin films and is a strong candidate for a number of applications. For example, it can be employed as an antireflection coating (ARC) on a silicon solar cell with a resultant increase in cell efficiency of approximately 21% or as a UV dosimeter.[23]

Experimental Section

Reagents. The benzoyltrifluoroacetone, benzoylacetone, and 2,2′-dipyridyl were obtained from Eastman Chemicals and were used without further purification. The Eu(NO$_3$)$_3$·6H$_2$O (99.9% Eu) was purchased from Rhône-Poulenc Basic Chemicals Co. All solvents used were of reagent quality.

Preparation of Complexes. The syntheses of Eu(btfa)$_3$·bipy and Eu(bzac)$_3$·bipy were accomplished by adding a stoichiometric quantity of an ethanolic solution of Eu(NO$_3$)$_3$·6H$_2$O (1 mmol) dropwise with stirring to an ethanolic solution containing the anion of the β-diketone (3 mmol) (btfa or bzac, prepared by neutralization with an aqueous solution of NaOH) and bipy (1 mmol) over a 2 h period. The compounds precipitated and were separated by filtration and washed with a small amount of ethanol. The white powders had melting points of 193−4 °C [Eu(btfa)$_3$·bipy] and 173−4 °C [Eu(bzac)$_3$·bipy]. Chemical analysis of the fluorinated compound confirmed its formulation (C calcd 50.58, found 50.26; H calcd 2.75, found 2.60; N calcd 2.94, found 2.92). Crystallization of Eu(btfa)$_3$·bipy from ethyl acetate/methanol gave crystals suitable for X-ray structure determination. The melting point and luminescence spectra of the powder and crystals were identical.

Spectral Measurements. Luminescence spectra were obtained on solid samples at room and liquid nitrogen temperatures in Duluth with a McPherson RS-10 spectrophotometer as described previously.[24] In

(6) Malta, O. L.; Couto dos Santos, M. A.; Thompson, L. C.; Ito, N. K. *J. Lumin.* **1996**, *69*, 77.
(7) Brecknell, D. J.; Raber, D. J.; Ferguson, D. M. *J. Mol. Struct. (THEOCHEM)* **1985**, *124*, 343.
(8) Ferguson, D. M.; Raber, D. J. *J. Comput. Chem.* **1990**, *11*, 1061.
(9) Hay, B. P. *Inorg. Chem.* **1991**, *30*, 2876.
(10) Fossheim, R.; Dugstad, H.; Dahl, G. *J. Med. Chem.* **1991**, *34*, 819.
(11) de Andrade, A. V. M.; da Costa, N. V., Jr.; Simas, A. M.; de Sá, G. F. *Chem. Phys. Lett.* **1994**, *227*, 349.
(12) de Andrade, A. V. M.; da Costa, N. V., Jr.; Simas, A. M.; de Sá, G. F. *J. Alloys Compd.* **1995**, *225*, 55.
(13) de Andrade, A. V. M.; Longo, R. L.; Simas, A. M.; de Sá, G. F. *J. Chem. Soc., Faraday Trans.* **1996**, *92*, 1835.
(14) Batista, H. J.; de Andrade, A. V. M.; Longo, R. L.; Simas, A. M.; de Sá, G. F.; Thompson, L. C. *J. Lumin.* **1997**, *72*−*74*, 159.
(15) Longo, R. L. Presented at the *17th Brazilian Symposium of Theoretical Chemistry*, Caxambu, Nov 17−19, 1997.
(16) Benson, M. T.; Cundari, T. R.; Lutz, M. L.; Sommerer, S. O. In *Reviews in Computational Chemistry*; Boyd, D., Lipkowitz, K., Eds.; VCH: New York, 1996, Vol. 8, pp 145−202.
(17) de Andrade, A. V. M.; da Costa, N. V., Jr.; Simas, A. M.; de Sá, G. F. Submitted for publication.
(18) Rocha, G. B.; Simas, A. M. Presented at the *17th Brazilian Symposium of Theoretical Chemistry*, Caxambu, Nov 17−19, 1997.
(19) Stewart, J. J. J. P. *MOPAC 93.00 Manual*; Fujitsu Limited: Tokyo, Japan, 1993; *J. Comput.-Aided Mol. Des.* **1990**, *4*, 1.
(20) Ridley, J. E.; Zerner, M. C. *Theor. Chim. Acta* **1973**, *32*, 111; **1976**, *42*, 223.
(21) Zerner, M. C.; Loew, G. H.; Kirchner, R. F.; Mueller-Westerhoff, U. T. *J. Am. Chem. Soc.* **1980**, *102*, 589.
(22) de Andrade, A. V. M.; da Costa, N. V., Jr.; Malta, O. L.; Longo, R. L.; Simas, A. M.; de Sá, G. F. *J. Alloys Compd.* **1997**, *250*, 412.
(23) (a) de Sá, G. F.; Alves, S., Jr.; da Silva, E. F., Jr. *Opt. Mater. (Amsterdam)*, in press. (b) Gameiro, C. G.; da Silva, E. F., Jr.; Alves, S., Jr.; de Sá, G. F.; Santa-Cruz, P. A. Submitted to Materials Science Forum.

Table 1. Crystallographic Data for $Eu(btfa)_3 \cdot bipy$

empirical formula: $EuC_{40}H_{26}O_6N_2F_9$	fw: 953.60
cryst syst: monoclinic	space group: $P2_1/n$ (No. 14)
$a = 11.122(5)$ Å	$T = 24 \pm 1$ °C
$b = 22.860(8)$ Å	$\lambda =$ Mo Kα (0.710 69 Å)
$c = 15.870(6)$ Å	$\rho_{calcd} = 1.609$ g/cm^3
$\beta = 102.62(3)°$	$\mu = 16.81$ mm^{-1}
$V = 3937(5)$ Å^3	$R = 0.052^a$
$Z = 4$	$R_w = 0.052^b$

$^a R = \sum(|F_o| - |F_c|)/\sum|F_o|$. $^b R_w = [(\sum w(|F_o| - |F_c|)^2/\sum w|F_o|^2)]^{1/2}$.

Recife, measurements of luminescence were made at both temperatures on a Jobin Yvon U1000 spectrophotometer and measurements of lifetime were made as described previously.[25] Absorption spectra in the UV region were obtained from ethanol solutions of the complexes ($\approx 10^{-4}-10^{-5}$ M) with a Perkin-Elmer Lambda 6 spectrophotometer. A UV spectrum of the fluorinated complex was also obtained in the solid state from a film of 400 Å thickness that was prepared by the thermal deposition of the complex on a quartz disk that had been previously cleaned and degreased to ensure proper film adhesion. The film was prepared by thermally evaporating the compound from an alumina crucible onto the substrate and defined by photolithography to form a rectangular structure with an area of about 1 cm^2. The thickness of the film was monitored during deposition by a quartz crystal thickness meter and, after deposition, ellipsometry measurements at several wavelengths to ensure film quality and uniformity. The luminescence spectrum and lifetime of the film were the same as those of analytically pure samples of the complex.

Structure Determination. The determination of the structure was carried out in the X-ray Crystallography Laboratory of the University of Minnesota—Twin Cities. Crystal data are summarized in Table 1, and full details of the structure determination are given in the Supporting Information. All intensity data were collected on an Enraf-Nonius CAD4 diffractometer using monochromated Mo Kα radiation. The intensities of three representative reflections that were measured after each 80 min period of exposure remained constant, indicating crystal and electronic stability. The structure was solved by direct methods as described previously[24] using the programs MITHRIL[26] and DIRDIF,[27] and all calculations were performed with the TEXSAN crystallographic software package of Molecular Structure Corporation.

Theoretical Calculations. The ground state geometries of both the fluorinated and nonfluorinated complexes were obtained using the SMLC/AM1 method with an improved parametrization.[17] In this model, the lanthanide ion is represented, within AM1,[28] by a sparkle which is a point of charge $+3e$ in the center of a repulsive spherical potential of the form $\exp(-\alpha r)$. As such, the sparkle model simulates well the essentially electrostatic interaction between the lanthanide ion and the ligands and the geometry of the entire complex (sparkle plus ligands) is optimized. In the first parametrization of the SMLC/AM1 model,[11-13] chemometric approaches, such as principal component analysis and factorial analysis, were used to obtain the optimum values for the parameter α (ALPAM1) and also for the monopole−monopole interaction parameter (AMAM1) involved in the core−core repulsion integrals. However, to improve the model and at the same time keep it consistent with the AM1 Hamiltonian, SMLC/AM1 has been generalized so that Gaussian functions similar to the ones used in AM1 to improve the core−core interaction were introduced and all six Gaussian parameters were optimized for several europium(III) compounds.[17] It should be noted that a proper description of complexes with cryptate and cagelike ligands was obtained only with the latter parametrization.

For the determination of the molecular structure of a new compound, several initial guesses for the starting geometry are used and the most stable solution is considered the appropriate structure. When the crystallographic structure is known for a similar compound, it is used as the initial guess for the geometry optimization procedure.

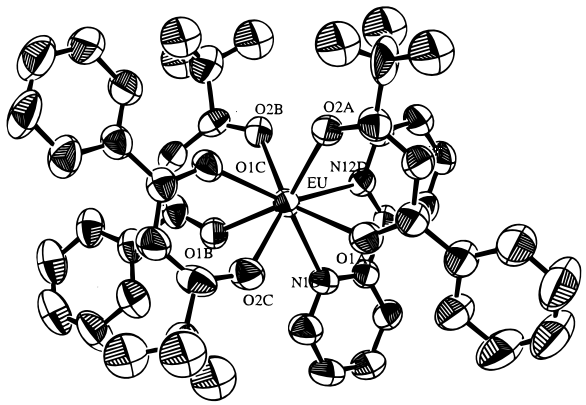

Figure 1. ORTEP drawing of $Eu(btfa)_3 \cdot bipy$ (50.0% probability ellipsoids).

The energy levels and transition moments were calculated with the INDO/S-CI method[20,21] implemented within the ZINDO program[29] allowing the comparison and prediction of the electronic absorption spectra. The molecular structure used was either from SMLC/AM1 model version 2 or from X-ray crystallography where the sparkle or the metal ion is replaced by a point of charge $+3e$.[13] Only the singly excited configurations (CIS) with respect to the closed shell reference are included in the CI matrix. These configurations are generated by all single substitutions, within a chosen set of occupied and unoccupied orbitals, on the reference determinant. The choice of this orbital set used to generate the CI configurations is made by saturating the CIS space in a given range of energy. That is, a preliminary electronic spectrum is generated from a small set of orbitals. This configuration space is then gradually increased until there are no visual differences between the spectra generated by two consecutive sets of configurations. The range of energy chosen for performing this visual comparison corresponds to 200−600 nm. Once the configuration space is selected for one complex or a set of ligands, it is used for similar complexes and/or ligands. In order to simulate the experimental electronic absorption spectra it is necessary to take into account the line broadening of the calculated transition energies and moments. This can be accomplished by considering that binary collisions are the main reason for this broadening in the condensed phase. Assuming that the collisions are strong and short enough that the Boltzmann distribution is restored after the collision, the Van Vleck−Weisskopf line shape function can be obtained,[30] of which the Lorentzian form is a particular case.[31] It should be noted that for frequencies in the UV−vis region there is no practical distinction between the Van Vleck−Weisskopf and Lorentzian line shapes. The calculated transition energies and oscillator strengths are then fitted and normalized to a Lorentzian line shape with a given half-height bandwidth (28 nm, in the present case). It should be noted that when the line shape function is transformed from the frequency to the wavelength domain, the intensities (oscillator strengths) become explicitly frequency dependent and the relative intensities can be very different when comparing the spectrum in these domains.

Results

Experimental Results. The compound $Eu(btfa)_3 \cdot bipy$ crystallizes in a monoclinic space group ($P2_1/n$) with four molecules in the unit cell. As expected, the complex is eight-coordinate with all six β-diketone oxygen atoms and the two nitrogen atoms from the dipyridyl bound to the metal (Figure 1). The average

(24) Holtz, R. C.; Thompson, L. C. *Inorg. Chem.* **1993**, *32*, 5251.
(25) de Sá, G. F.; de Azevedo, W. M.; Gomes, A. S. L. *J. Chem. Res.* **1994**, 234.
(26) Gilmore, C. J. *J. Appl. Crystallogr.* **1984**, *17*, 42.
(27) Beurskens, P. T. *Technical Report 1984/1*, Crystallography Laboratory, Toernooiveld, 6525 Ed.: Nijmegen, The Netherlands.
(28) Dewar, M. J. S.; Zoebish, E. G.; Healy E. F.; Stewart, J. J. P. *J. Am. Chem. Soc.* **1985**, *107*, 3902.
(29) Zerner, M. C. *ZINDO Manual*; QTP—University of Florida: Gainesville, FL, 1990.
(30) Van Vleck, J. H.; Weisskopf, V. F. *Rev. Mod. Phys.* **1945**, *17*, 227.
(31) Townes, C. H.; Schawlow, A. L. *Microwave Spectroscopy*; Dover: New York, 1975.

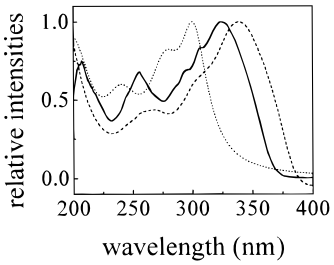

Figure 2. Calculated electronic absorption spectrum of Eu(btfa)$_3$·bipy (SMLC input geometry) (dotted line); ethanolic solution (solid line); thin film on a quartz disk (dashed line).

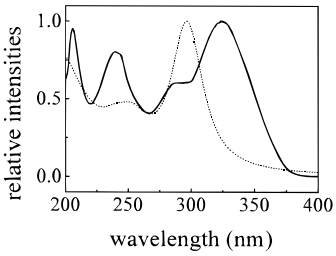

Figure 3. Calculated electronic spectrum of Eu(bzac)$_3$·bipy (dotted line); ethanolic solution (solid line).

Eu−O distance of 2.360(19) Å and the average Eu−N distance of 2.582(5) Å are typical for complexes of this type. The CF_3 groups are commonly disordered in substituted β-diketone complexes, and such is the case in this complex. However, this did not affect the solution of the structure. Visual inspection suggests that the coordination polyhedron is a square antiprism. This was confirmed by an analysis using the method developed by Porai-Koshits and Aslanov,[32] although there are significant deviations from the ideal values. The two "square" planes are defined by O2C, O1C, O2A, and O1A and by O1B, O2B, N12D, and N1D, respectively.

The electronic absorption spectra of the fluorinated complex in the region 200−400 nm, both in ethanol solution and as a thin film, are shown in Figure 2, and that of the nonfluorinated complex in ethanol solution is shown in Figure 3. The most intense peak occurs in all three cases between 325 and 350 nm. The calculated gas phase spectrum for each complex is also shown in Figure 2 and Figure 3. The spectra are normalized to the same arbitrary scale, but the molar absorptivities are 2.6 $\times$ 10^4 l mol^{-1} cm^{-1} for the fluorinated complex and 1.2 $\times$ 10^4 l mol^{-1} cm^{-1} for the nonfluorinated complex.

The complex Eu(btfa)$_3$·bipy is very strongly luminescent in the red when excited with near-ultraviolet radiation, and transitions were measured from the first excited level to the first five components of the ground term (Figure 4). The main emission occurs, as expected, in the $^5D_0 \rightarrow {}^7F_2$ transition. Although the $^5D_0 \rightarrow {}^7F_0$ and $^5D_0 \rightarrow {}^7F_1$ transitions also are present, they are 50 and 10 times less intense, respectively. The $^5D_0 \rightarrow {}^7F_0$ transition is a singlet, which indicates the presence of only a single emitting species, and the degeneracy of the $J = 1$ and $J = 2$ levels is completely removed, in agreement with the structural results. There is no indication of emission from the higher excited levels such as $^5D_1$. The emission spectrum of Eu(bzac)$_3$·bipy is similar except that the transitions $^5D_0 \rightarrow {}^7F_0$ and $^5D_0 \rightarrow {}^7F_1$ are now both about 10 times less intense than the $^5D_0 \rightarrow {}^7F_2$ transition.

Theoretical Results and Discussion. Because the structure of Eu(btfa)$_3$·bipy had been determined by X-ray diffraction, this geometry was used as the input to the SMLC/AM1 method. The output geometry conformed very well to the experimental geometry, and the values determined for the Eu−O and Eu−N distances along with the angles about the europium(III) ion are presented in Table 2. The average predicted values for the Eu−O and Eu−N distances are 2.38 and 2.54 Å, and the average deviation of all eight values from the experimental values in the solid state is 0.05 Å. The data for the bond angles show a similarly good agreement. No experimental structure is available for Eu(bzac)$_3$·bipy, and its ground state geometry was predicted by means of the SMLC/AM1 method using the geometry of the fluorinated complex as the input. The two structures predicted by the SMLC/AM1 method are compared

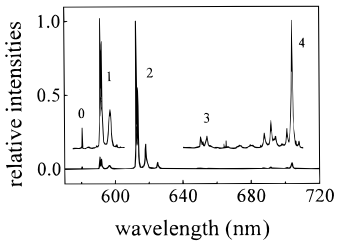

Figure 4. Luminescence spectrum of Eu(btfa)$_3$·bipy at 77 K upon ligand excitation (370 nm). The labels refer to the J values of the final level of the emission transition $^5D_0 \rightarrow {}^7F_J$. The two insets show the $^5D_0 \rightarrow {}^7F_{0,1}$ and the $^5D_0 \rightarrow {}^7F_{3,4}$ regions magnified but not in the same scale.

Table 2. Interatomic Distances and Angles between the Atoms of the Coordination Polyhedron and the Eu(III) Ion for the Eu(btfa)$_3$·bipy (FL) and Eu(bzac)$_3$·bipy (NFL)

	exptl	calcd	
	FL	FL	NFL
	Distances (Å)		
Eu−O1A	2.369(5)	2.407	2.383
Eu−O2A	2.351(5)	2.388	2.357
Eu−O1B	2.399(5)	2.362	2.353
Eu−O2B	2.349(6)	2.431	2.406
Eu−O1C	2.369(5)	2.350	2.354
Eu−O2C	2.321(5)	2.388	2.376
Eu−N1D	2.586(6)	2.560	2.633
Eu−N12D	2.577(5)	2.531	2.582
	Angles (deg)		
O1A-Eu−O2A	71.1(2)	65.8	66.5
O1A-Eu−O1B	140.0(2)	144.9	145.6
O1A-Eu−O2B	141.3(2)	141.1	134.9
O1A-Eu−O1C	123.9(2)	117.5	113.8
O1A-Eu−O2C	79.4(2)	82.5	81.2
O1A-Eu−N1D	71.3(2)	73.0	73.1
O1A-Eu−N12D	76.4(2)	78.5	74.9
O2A-Eu−O1B	148.8(2)	149.2	146.2
O2A-Eu−O2B	82.8(2)	85.7	80.3
O2A-Eu−O1C	78.8(2)	82.3	80.9
O2A-Eu−O2C	115.2(2)	118.2	120.3
O2A-Eu−N1D	133.6(2)	131.8	132.6
O2A-Eu−N12D	83.0(2)	81.6	81.8
O1B−Eu−O2B	71.4(2)	66.2	67.4
O1B−Eu−O1C	78.3(2)	81.6	88.4
O1B−Eu−O2C	77.0(2)	78.6	83.9
O1B−Eu−N1D	74.0(2)	74.4	73.2
O1B−Eu−N12D	104.6(2)	99.8	96.1
O2B−Eu−O1C	75.8(2)	81.9	88.7
O2B−Eu−O2C	138.7(2)	135.9	143.6
O2B−Eu−N1D	111.9(2)	114.2	114.8
O2B−Eu−N12D	72.4(2)	71.3	70.7
O1C−Eu−O2C	72.3(2)	66.9	67.8
O1C−Eu−N1D	146.4(2)	141.0	139.8
O1C−Eu−N12D	145.0(2)	149.6	155.1
O2C−Eu−N1D	83.1(2)	78.5	74.8
O2C−Eu−N12D	142.7(2)	143.4	137.0
N1D-Eu−N12D	62.5(2)	66.2	64.3

(32) Porai-Koshits, M. A.; Aslanov, L. A. *J. Struct. Chem.* **1972**, *13*, 244.

also in Table 2, and it can be seen that they are very similar, suggesting that the effect of fluorination on the ground state structure is minimal. With the exception of the Eu−O3A distance, the Eu−O distances are slightly shorter in the nonfluorinated complex whereas the Eu−N distances are calculated to be slightly longer. This slightly shorter Eu−N distance in compounds containing the CF_3 group, compared to compounds that do not, has been observed in the X-ray structures of 10 related molecules of this same type, six of which contain the CF_3 group.[33] As can be seen in Table 2, this shortening of the Eu−N distance in Eu(btfa)$_3$·bipy is 0.05−0.08 Å whereas the lengthening of the Eu−O distances is ∼ 0.02 Å.

The UV absorption spectra of the fluorinated and nonfluorinated complexes calculated via INDO/S-CI (Figures 2 and 3) are in satisfactory agreement with the experimental spectra obtained from ethanol solution. It has been shown previously[14] that the use of the calculated molecular structure (SMLC/AM1) as the input geometry for the spectroscopic calculation yields better agreement with the experimental spectra than the spectra calculated with the crystallographic structure. Both qualitative (number of maxima and shoulders) and quantitative features of the absorption spectra are reproduced, and a systematic blue shift of 20 nm in the calculated spectra is found when compared to the experimental one. This shift might be due to several effects, but mainly from the neglect of the solvent effects in the calculated spectra.

Also in Figure 2 is the absorption spectrum obtained from the thin film. This is quite similar to the solution spectrum and, thus, to that calculated from the SMLC/AM1 geometry. The number of peaks and their relative intensities are again reproduced fairly well. The experimental spectrum is shifted toward the red relative to that of the isolated gaseous molecule even more than in the case of the solvated molecules. This additional crystal lattice effect is quite reasonable. It would be desirable to have the spectrum of the molecule in the gas phase for direct comparison with the theoretical spectrum, but this is not presently available. The volatility of some adducts of the tris-β-diketonates has made it possible to determine their gas phase luminescence spectra, and in the future we hope to be able to measure the corresponding absorption spectra of molecules of this type.

The fluorinated complex is visually considerably more luminescent than the nonfluorinated complex. This is quantitatively reflected in the quantum yield of 65% for Eu(btfa)$_3$·bipy, both in the solid state and in the thin film, compared to 16% for solid Eu(bzac)$_3$·bipy. Although our ultimate intention is to analyze the quantum yields in these compounds using the method described in ref 34 we can make a number of qualitative observations from the calculated spectra that are in agreement with the experimental values.

The origin of the triplet donor states of the ligands is very important, because it can have a profound influence on the energy transfer rate. The lowest triplet state in the fluorinated complex (23 938 cm^{-1}) is basically centered at the bipy ligand whereas in the nonfluorinated complex this (25 260 cm^{-1}) is the second lowest level. Both of these levels have similar atomic contributions. In both complexes, almost all of the other triplet states are due to the β-diketone ligands and have similar atomic compositions. Moreover, fluorination seems to lower the triplet state energies overall, of an amount of approximately 1000 cm^{-1}, yielding donor states in closer resonance with the metal ion acceptor states ($^5D_2$: 21 483 cm^{-1}); see the Supporting Information for a complete table of energy levels. According to the Fermi golden rule the energy transfer rate (W_{ET}) can be written in the form[35]

$$W_{ET} = \frac{2\pi}{\hbar}|\langle\Psi_f\phi_f|H|\Psi_i\phi_i\rangle|^2 F = \frac{2\pi}{\hbar}|H_{da}|^2 F$$

where the donor−acceptor matrix element (H_{da}) has the following dependence with the donor−acceptor distance (R_L):

$$|H_{da}|^2 \propto \frac{1}{(R_L^{l+2})^2}$$

with l varying from 1 up to the highest angular momentum value allowed by the selection rules for the 4f electrons, usually 6. The energy and temperature dependence is included in the F term, which contains a summation over the Franck−Condon factor and the appropriate energy mismatch conditions. Assuming that the ligand bandwidth (γ_L) is much larger than that for the rare earth ion, it can be shown[35] that

$$F = \frac{1}{\gamma_L}\sqrt{\frac{\ln 2}{\pi}}\exp\left[-\left(\frac{\Delta}{\gamma_L}\right)^2 \ln 2\right]$$

where $\Delta = E_L - E_{RE}$ is the energy difference between the donor and acceptor band peaks.

Upon fluorination, the donor−acceptor distance changes (decreases approximately 0.07 Å). The ratio between the electronic factors of the fluorinated (FL) and nonfluorinated (NF) complexes can then be written approximately as

$$\frac{|H_{da}|_{FL}^2}{|H_{da}|_{NF}^2} \approx \left[\frac{R_L^{NF}}{R_L^{FL}}\right]^{2l+4}$$

For a typical value of 5 Å for the bipy−Ln(III) distance in the nonfluorinated complex, the same distance in the fluorinated complex is shortened to 4.93 Å, and this ratio is 1.09 and 1.12 for $l = 1$ and 2, respectively. Similarly, the ratio for the mismatch energy factor is given by

$$\frac{F_{FL}}{F_{NF}} = \exp\left[\frac{\ln 2}{\gamma_L^2}[(\Delta_{NF})^2 - (\Delta_{FL})^2]\right]$$

which for a typical value of 5000 cm^{-1} for γ_L yields 1.41 and 1.21 for the lowest triplet donor state to the $^5D_1$ and $^5D_2$ acceptor states, respectively. The ratio between the energy transfer rates should then be in the range 1.32−1.58, showing that those two effects, namely, lowering the donor state energy and shortening the donor−acceptor distance, are important in explaining the significant increase in the luminescence quantum yield (16% to 65%) when the CH_3 groups are replaced by CF_3 in the europium complex.

It is well accepted that the nonradiative deactivation of the ligand and metal ion excited states by vibronic coupling with O−H modes is effective in quenching the fluorescence, thus

(33) Thompson, L. C.; Young, V. G.; Berry, S.; Atchison, F. W.; Maser, D. Unpublished results.

(34) (a) de Mello Donegá, C.; Ribeiro, S. J. L.; Gonçalves, R. R.; Blasse, G. *J. Phys. Chem. Solids* **1996**, *57*, 1727. (b) de Mello Donegá, C.; Alves, S., Jr.; de Sá, G. F. *J. Chem. Soc., Chem. Commun.* **1996**, 1199.

(35) Malta, O. L. *J. Lumin.* **1997**, *71*, 229.

decreasing the quantum yield. It has been proposed[36] that the vibronic coupling with C−H modes from CH_3 groups would also be effective, because the C−H stretching mode has a vibrational frequency close to that of the O−H. Therefore, it is very likely that the fluorination of the CH_3 groups will lead to a less effective vibronic coupling because of the significant difference between the vibrational frequencies of the C−F and C−H stretching modes.

Conclusions

The complex Eu(btfa)$_3$·bipy has been shown by X-ray diffraction to consist of a single species in agreement with the presence of a single $^5D_0 \rightarrow {}^7F_0$ line in the luminescence spectrum. The sparkle model, SMLC/AM1, gives a reasonably good prediction of the structure of the molecule, taking into account the differences between the gas and solid phases. Moreover, the method yields a similar structure for the analogous molecule Eu(bzac)$_3$·bipy. For both complexes the UV absorption spectrum determined by means of the INDO/S-CI technique is in satisfactory agreement with experiment.

The theoretical calculations of the molecular structure and the electronic energy levels have cast some light onto the origin of the significant increase of the luminescence quantum yield when the CH_3 groups are replaced by CF_3 groups in the Eu(bzac)$_3$·bipy complex. Indeed, there seem to be three factors acting in concert to increase the efficiency of the luminescence process, namely, a decrease in the donor−acceptor energy difference, a decrease in the donor−acceptor distance, and a decrease in the vibronic coupling with the C−F vibrational modes.

Acknowledgment. The authors are grateful to CNPq, PADCT, CAPES, FACEPE, and FINEP (Brazilian agencies) and to the Graduate School of the University of Minnesota for financial support, to Prof. Oscar Malta for useful suggestions, to Prof. Eronides Felisberto for the preparation of the thin film sample, to Mr. Severino Alves for spectroscopic measurements, and to Prof. Doyle Britton for the structure determination.

Supporting Information Available: Text describing data collection, data reduction, and structure solution and refinements and tables listing crystal data, intensity measurements, structure refinement details, positional and thermal parameters, general temperature factor expressions, bond distances, bond angles, torsional angles, intermolecula contacts, least-squares planes, and theoretical electronic energy levels for the complexes (45 pages). Ordering information is given on any current masthead page.

IC971602V

(36) (a) Bünzli, J.-C. G. In *Lanthanide Probes in Life, Chemical and Earth Sciences. Theory and Practice*; Bünzli, J.-C. G., Choppin, G. R., Eds.; Elsevier-North Holland: Amsterdam, 1989; Chapter 7. (b) Wang, Z.-M.; Choppin, G. R.; di Bernardo, P.; Zanonato, P.-L.; Portanova, R.; Tollazzi, M. *J. Chem. Soc., Dalton Trans.* **1993**, 2791.